N87-26706

1986

NASA/ASEE SUMMER FACULTY RESEARCH FELLOWSHIP PROGRAM

Johnson Space Center

University of Houston

A Comparison of Two Conformal Mapping Techniques Applied to an Aerobrake Body

Prepared by: Dr. Mark J. Hommel, P.E.

Academic Rank: Associate Professor

University   Prairie View A&M University
& Department: Department of Mechanical
                         Engineering

NASA/JSC
Directorate: Engineering

Division: Advanced Programs Office

Branch: Aerosciences

JSC Colleague: Dr. C.P. Li

Date: August 8, 1986

A COMPARISON OF TWO CONFORMAL MAPPING TECHNIQUES
APPLIED TO AN AEROBRAKE BODY

Conformal mapping is a classical technique which has been utilized for solving problems in aerodynamics and hydrodynamics for many years. Conformal mapping has been successfully applied in the construction of grids around airfoils, engine inlets and other aircraft configurations. These shapes are transformed onto a near-circle image for which the equations of fluid motion are discretized on the mapped plane and solved numerically by utilizing the appropriate techniques. In comparison to other grid-generation techniques such as algebraic or differential type, conformal mapping offers an analytical and accurate form even if the grid deformation is large. One of the most appealing features is that the grid can be constrained to remain orthogonal to the body after the transformation. Hence, the grid is suitable for analyzing the supersonic flow past a blunt object. The associated shock as a coordinate surface adjusts its position in the course of computation until convegence is reached.

In the present study, conformal mapping techniques have been applied to an Aerobrake Body having an axis of symmetry. Two different approaches have been utilized:
    (1) Karman-Trefftz Transformation
    (2) Point-Wise Schwarz-Christoffel Transformation
In both cases, the Aerobrake Body was mapped onto a near-circle, and a grid was generated in the mapped plane. The mapped body and grid were then mapped back into physical space and the properties of the associated grids were examined. Advantages and disadvantages of both approaches were discerned.

1. Introduction

A problem of interest to NASA involves the hypersonic flow past an aerobraking orbital transfer vehicle. As summarized by Li (1), several schemes have been utilized to simplify the numerical treatment of the problem. A primary simplification involves the mapping of the characteristic mushroom shape of the aerobrake vehicle onto a near-circle, generating a grid, solving the Navier-Stokes equations in the mapped plane, and subsequently mapping the solution back into physical space.

In examining the features of the grids generated by this procedure, competitive alternative methods have been re-discovered from elementary complex number theory. The two complementary methods of interest in the present study are as follows:

(1) Karman-Trefftz Transformation

(2) Point-wise Schwarz-Christoffel Transformation.

In the following brief report, both transformations are examined with respect to their suitability for transforming the aerobrake vehicle to a shape suitable for an existing Navier-Stokes computer code, and conclusions and recommendations regarding the two transformations are made. Finally, in order to gain deeper insight into the transformations, a simple square is also transformed by both methods, and the resulting grids examined as well.

2. Karman-Trefftz Transformation

The Karman-Trefftz transformation, which maps the z-plane into the w-plane, is given by the following relationship:

$$\frac{w-1}{w+1} = \left(\frac{z-h}{z+h^{*}}\right)^{\delta} \qquad (1)$$

where z represents the complex physical plane x+iy; w represents the complex mapped plane u+iv; δ is a real number to be defined below; and h is a "hinge point," which is a point in the vicinity of some point of interest on the body being transformed. The transformation has the property of smoothing out corners on the physical body, facilitating the generation of a grid around the body. Each sharp corner on the body is smoothed out in turn by repeated applications of the current transformation to every point on the body, each transformation having a specific value of h and δ. The real number δ is evaluated as follows:

$$\delta = \frac{\pi}{2\pi - \alpha_{int}} \qquad (2)$$

where α_{int} is the interior angle formed at a given corner of the physical body. Following Moretti (2), repeated applications of the transformation are applied in order of increasing δ. In the following figures, transformations are applied to a mushroom-shaped Aerobrake Body. Note in particular the values for h and δ for each transformation. Also note that the actual grid is generated in the mapped plane, where the body has come to resemble a near-circle, by constructing equiangularly spaced radial lines and their orthogonal complements. The grid and body are then mapped back into physical space by reversing the transformations. The computer program for this process is listed in Appendix 1.

Figure 1 shows the initial mushroom configuration, with the sharp corners numbered in the order to be transformed. Note that the first angle to be transformed is the perpendicular angle at point 1, so the exponent in the transformation is 2/3. The result of this first transformation is given in Figure 2, where the the sharp angles at points 2 and 3 are seen to persist, but the corner at point 1 has now been smoothed out. Again the perpendicular corner at 2 is chosen, so the exponent is 2/3, and the result of this transformation is shown in Figure 3. Finally, the corner at point 3 is transformed by using an exponent of 2, and the near-circle of Figure 4 is obtained.
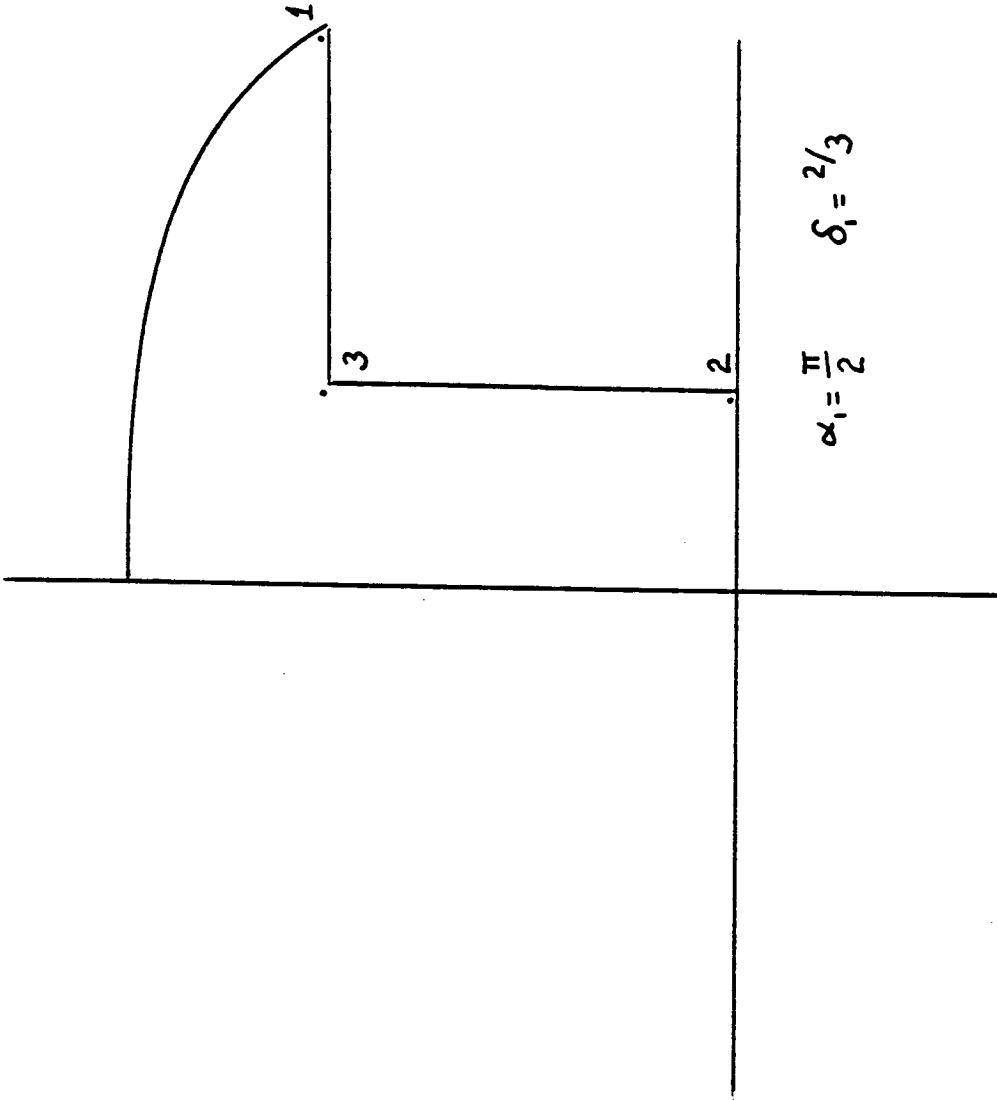
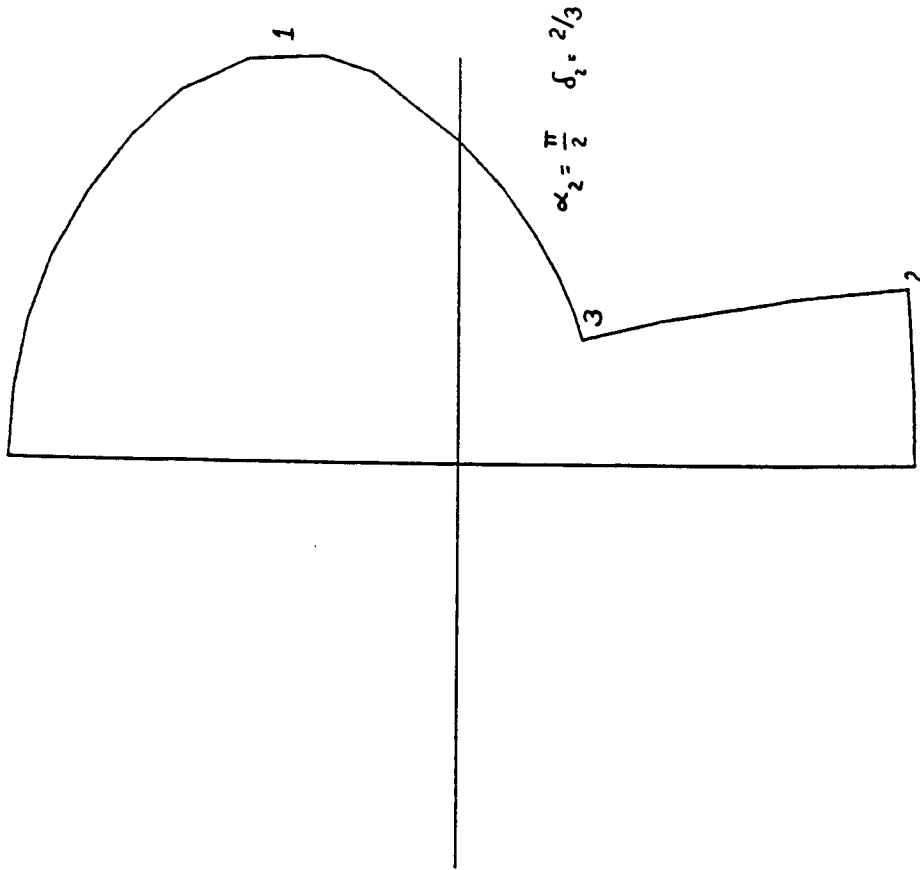Figure 1--Mushroom Configuration for Karman-Trefftz Transformation

$$\alpha_1 = \frac{\pi}{2} \qquad \delta_1 = \frac{2}{3}$$

$$\alpha_2 = \frac{\pi}{2} \qquad \delta_2 = 2/3$$

Figure 2--Result of First Transformation

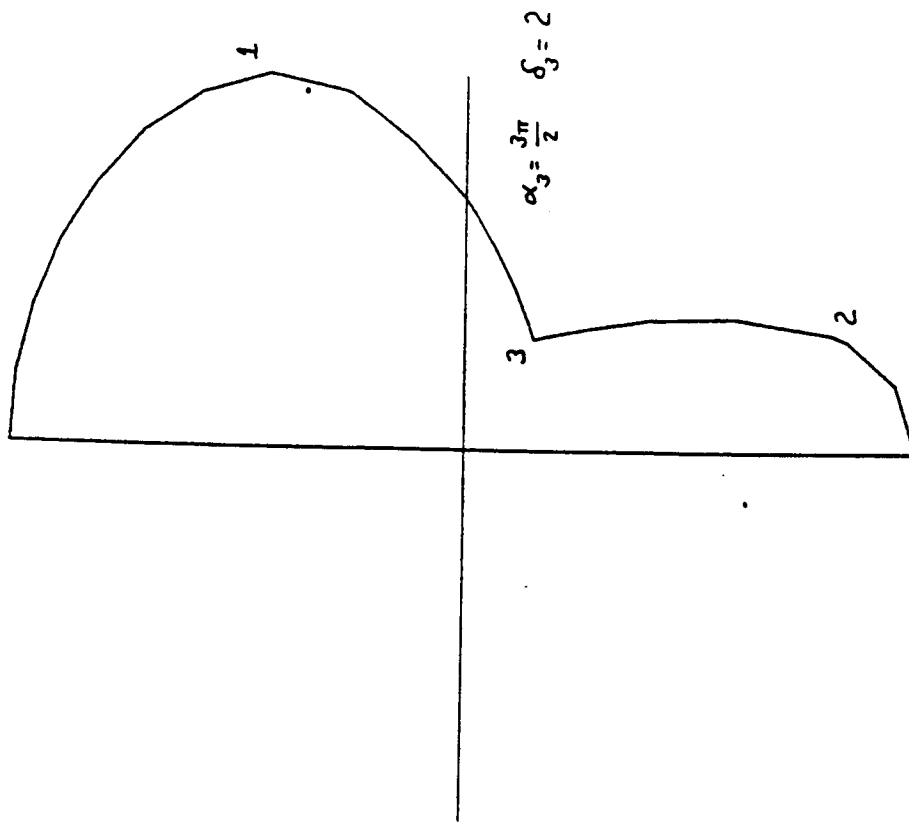$$\alpha_3 = \frac{3\pi}{2} \qquad \delta_3 = 2$$
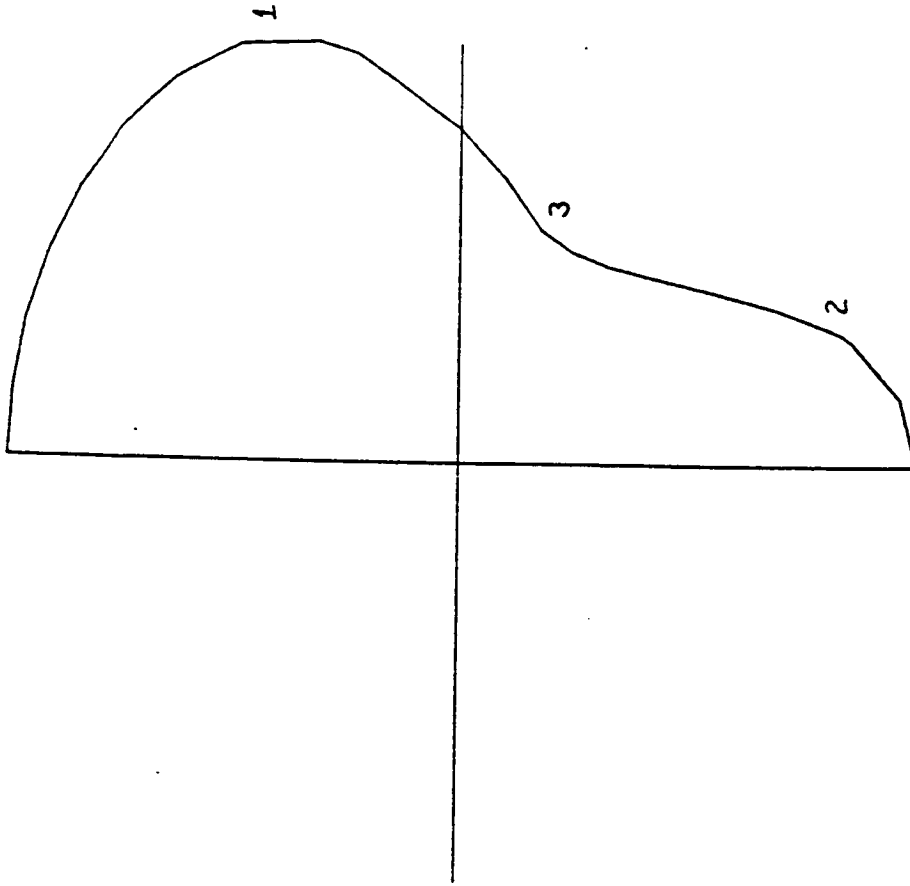
Figure 3--Result of Second Transformation

Figure 4--Near-Circle

Next, equi-angular radial lines are constructed from the origin, as well as their orthogonal complements, as shown in Figure 5. It is this set of points which are mapped back into the physical plane to become the grid in physical space. At this point, moreover, it is envisioned that the flow past the Aerobrake body could be obtained numerically, utilizing an existing Navier-Stokes computer code. Figures 6-8 show the resulting mesh in physical at successively improved levels of refinement.
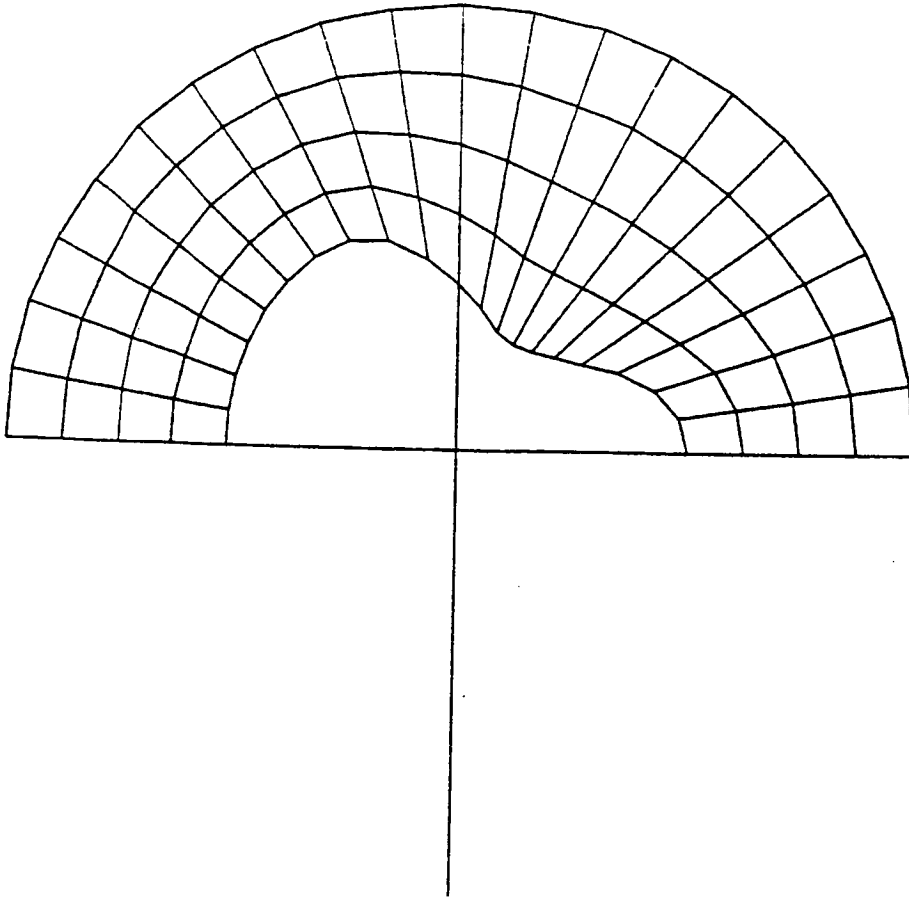
Figure 5--Karman-Trefftz Grid Construction
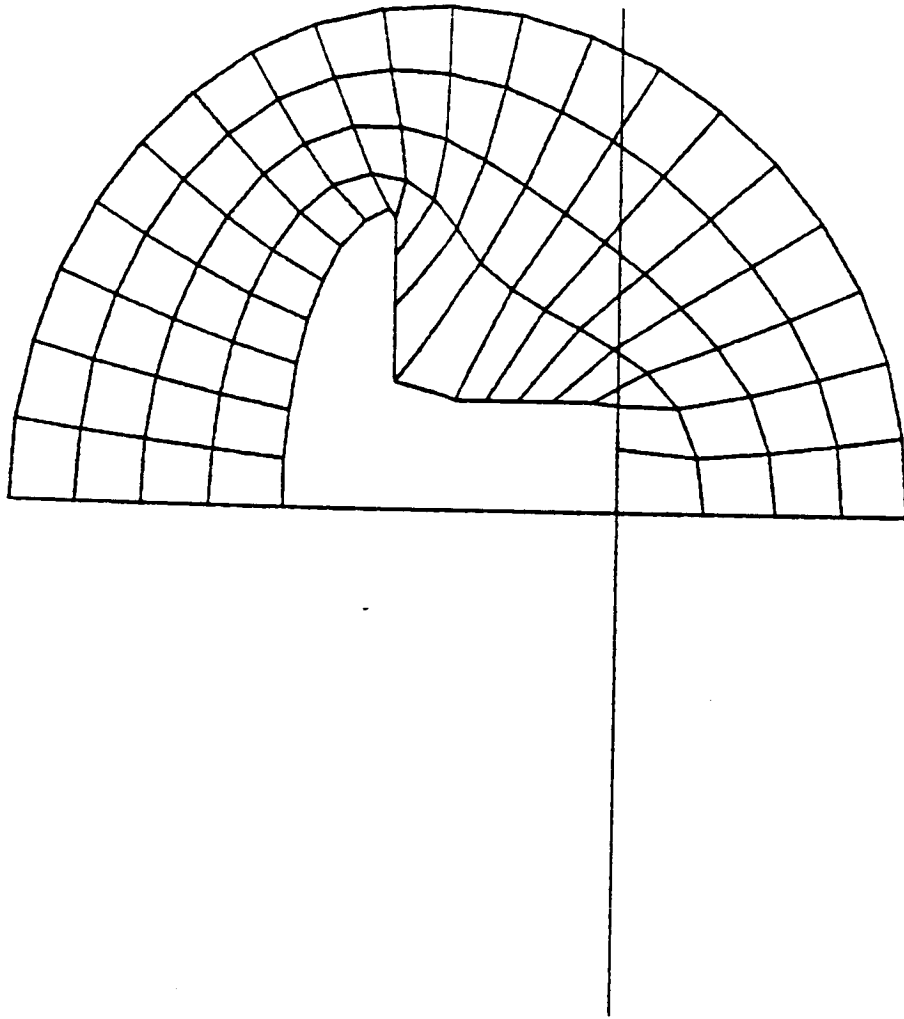
Figure 6--Grid in Physical Plane, Coarse Mesh

14-11
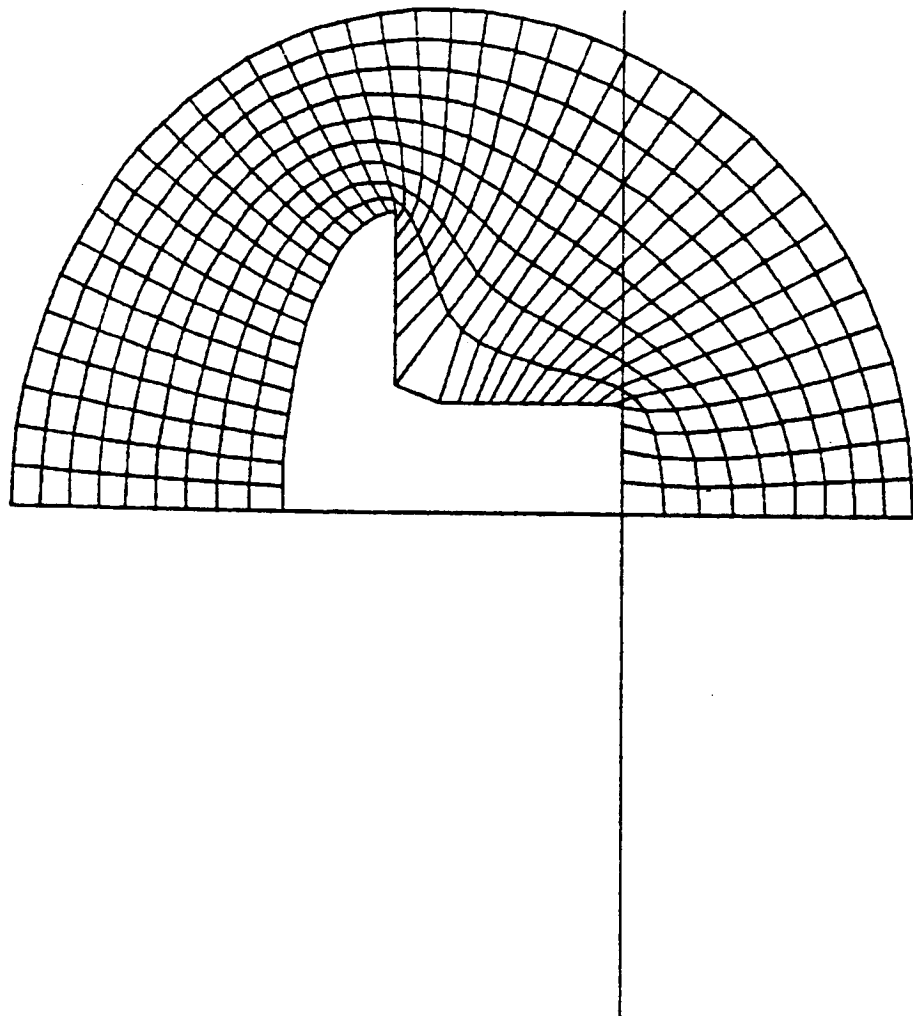
Figure 7--Grid in Physical Plane, Intermediate Mesh
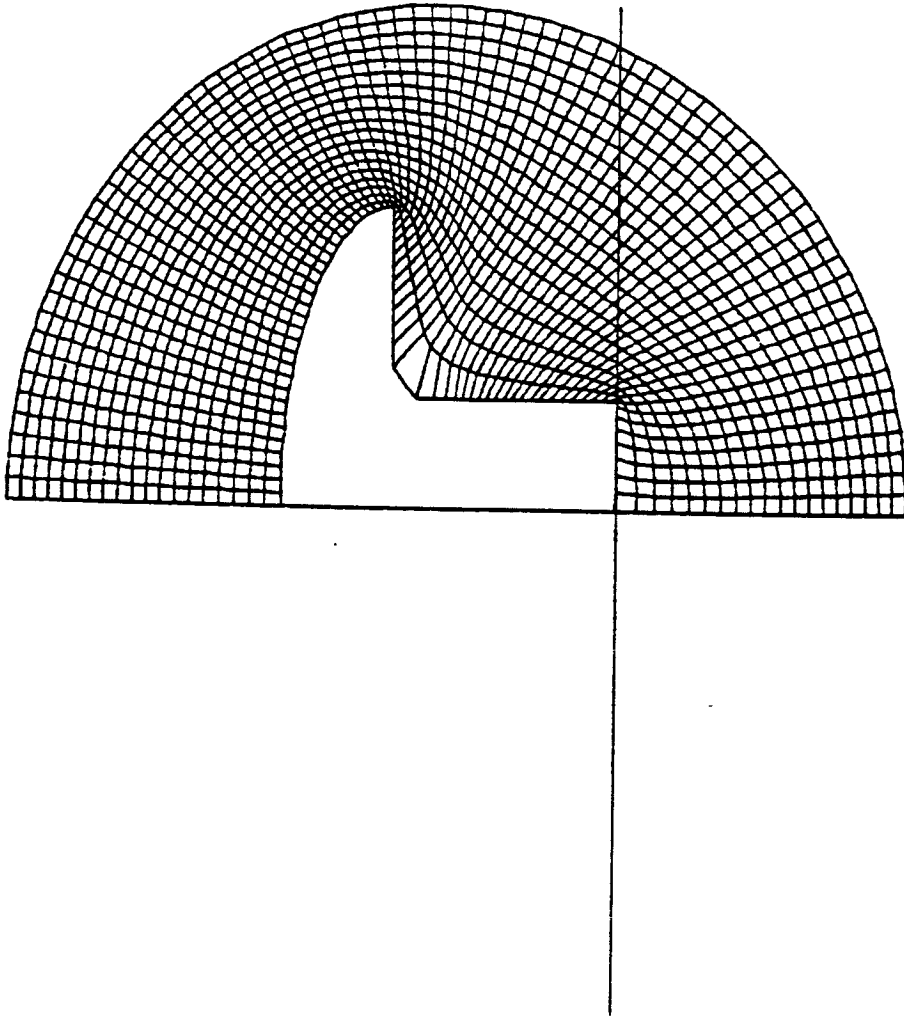
Figure 8--Grid in Physical Plane, Fine Mesh

3. Schwarz-Christoffel Transformation

The basic idea for an alternative transformation is presented by Hall (3), who refers to it as a "point-wise Schwarz-Christoffel transformation." Strictly speaking, however, the transformation is simply a power-law transformation taken from elementary complex number theory (Spiegel (4)). Motivation for the transformation is presented in Figure 9, where it is seen that points on the positive real axis in the physical plane remain on the real axis in the mapped plane, while points lying on a ray at angle in the physical plane are mapped onto the negative real axis in the mapped plane. Repeated applications of the transformation to every point on the physical body allows the mapping of the physical body onto the real axis. Finally, a grid can be generated in the mapped plane and mapped back into physical space using the inverse transformations. However, unlike the Karman-Trefftz transformation, the utilization of polar coordinates in the mapped plane for grid generation was found to provide inferior grid properties compared with the use of Cartesian coordinates in the mapped plane, because the axes in the mapped space do not correspond to 0=0 and in the physical space. The following figures show that the grid generated is of no practical use. A listing of the computer program utilized for the Schwarz-Christoffel transformation is given in Appendix 2.

Figure 10 shows the Aerobrake body in its initial orientation. It has been rotated with respect to Figure 1 so that the exponent in Figure 9 will be finite. The computer program then calculates the angle which a line from point 0 to point 1 makes with the real axis, and calculates the exponent for the first transformation. This transformation results in the moving of point 1 to the real axis, as shown in Figure 11. Note that point 2 has been "lost" in Figure 11, due to interpolation. A more refined representation of the body shows that this error can be made arbitrarily small. Alternatively, an improved interpolation routine will eliminate this problem altogether. Next, point 2 is brought up to the real axis, as shown in Figure 12, followed by the positioning of point 3 on the real axis, as shown in Figure 13. Finally, point 4 is brought up to the real axis by yet another transformation, whereupon the Kutta-Joukowsky transformation is applied to map the transformed body onto a near-circle, as shown in Figure 14. Now equi-angular radial lines and their orthogonal complements are constructed, as shown in Figure 15. Now, however, when the resulting grid is mapped back into the physical plane, the grid is seen to overlap into the lower half plane, as shown in Figure 16. This is clearly an unacceptable grid for computation.
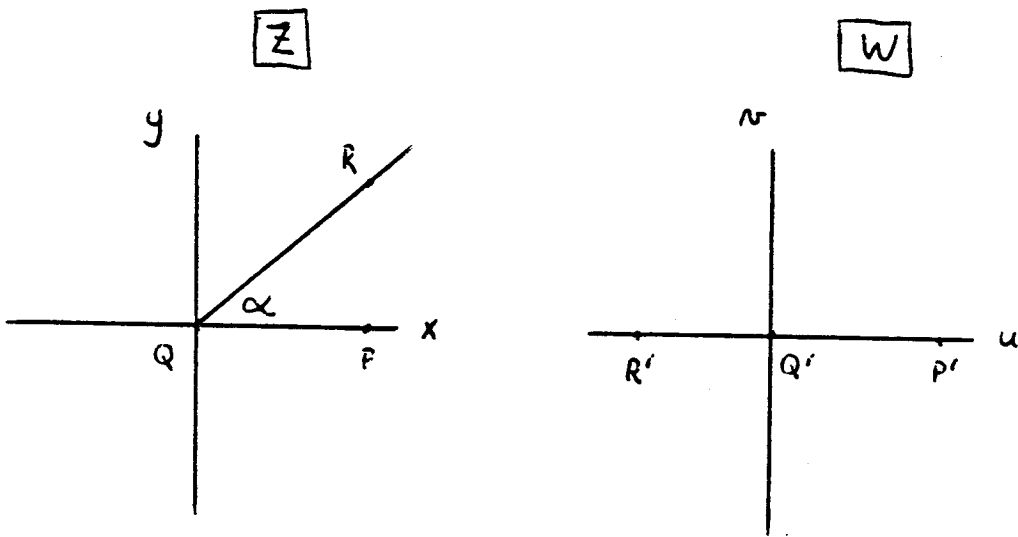
$$W = Z^{\pi/\alpha}$$

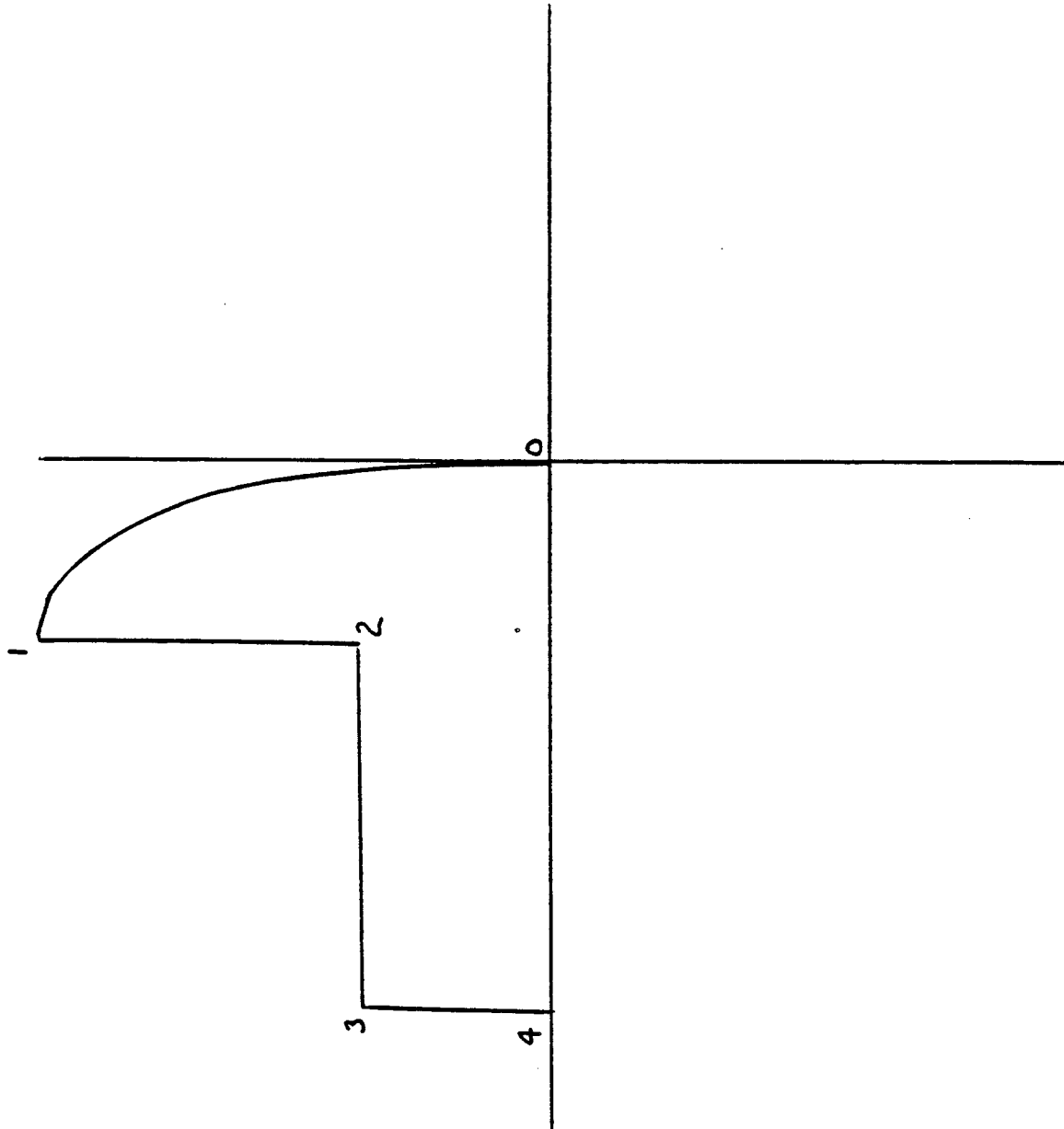Figure 9--Power Law Transformation

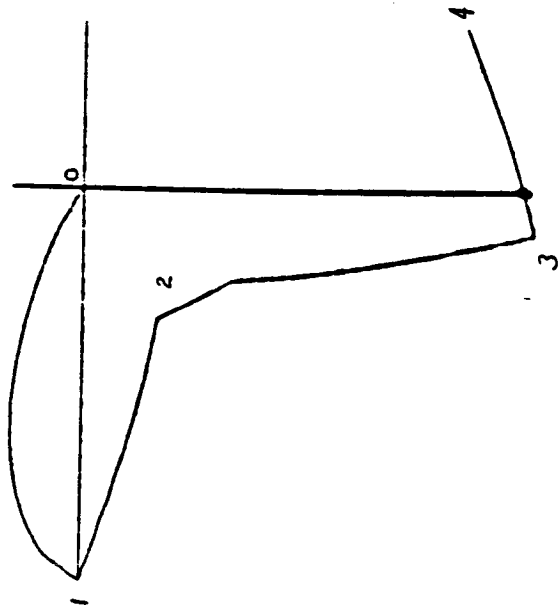Figure 10—Mushroom Orientation for Point-Wise Schwarz-Christoffel Transformation
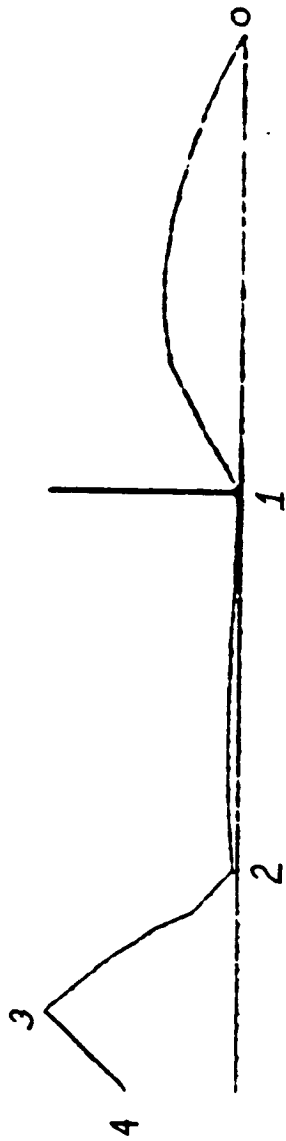
Figure 11--Result of First Transformation

Figure 12--Result of Second Transformation

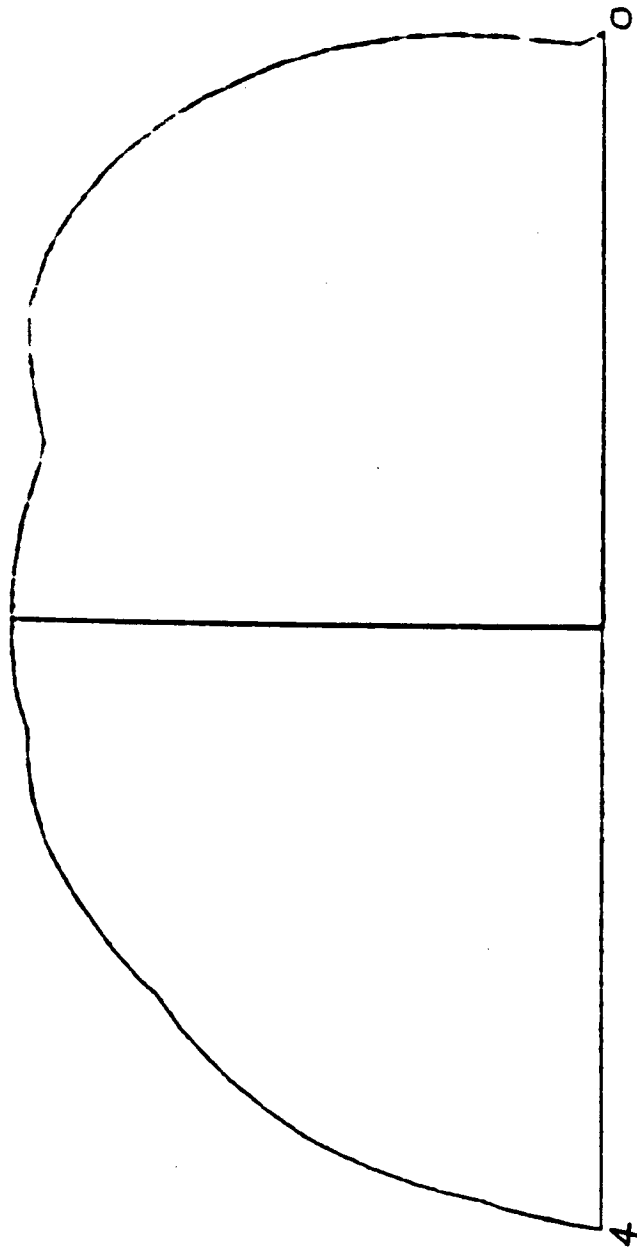Figure 13--Result of Third Transformation

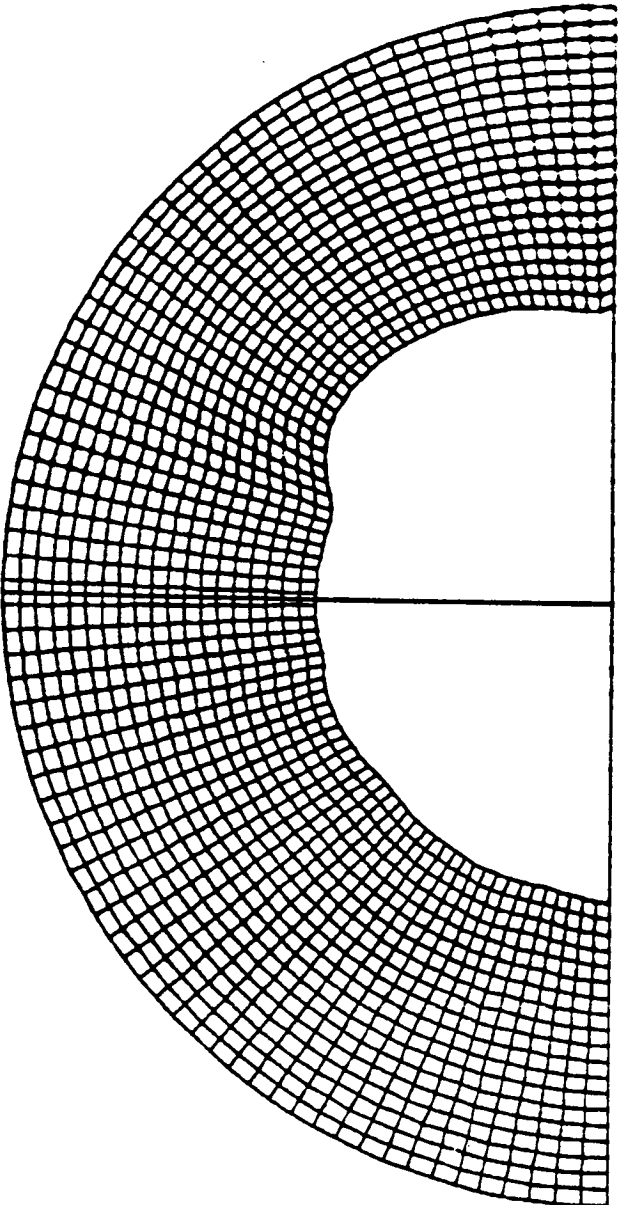Fig. 14 – – After Applying Kutta-Joukowsky Transformation
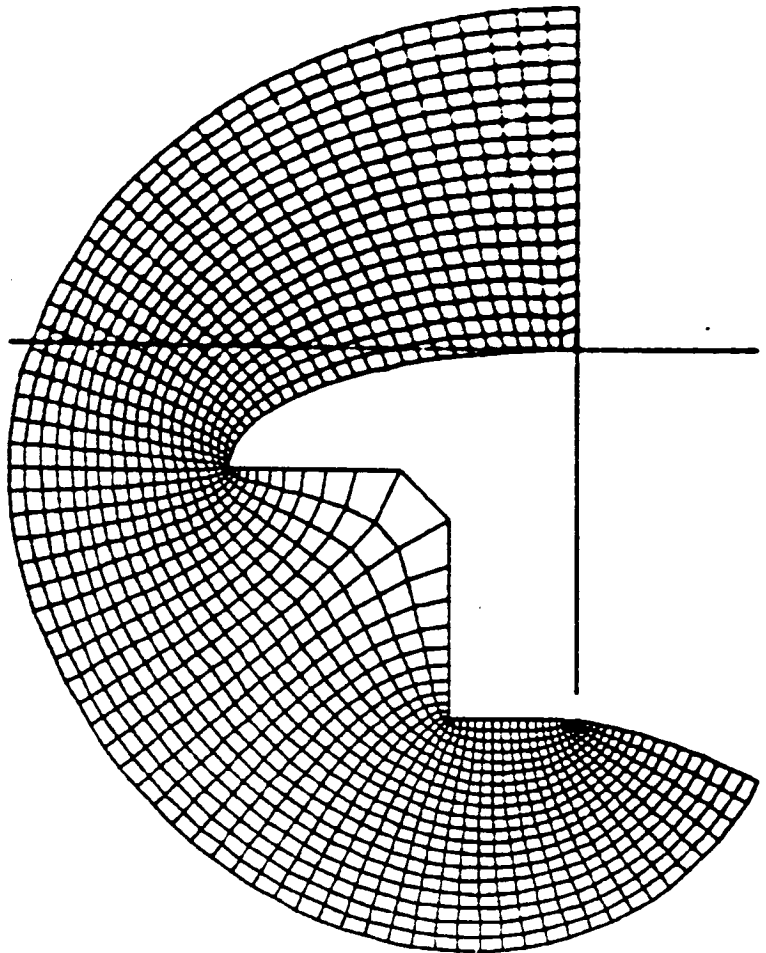
Figure 15--Grid Construction in Mapped Plane

DEN= 0.20915E+01

DEN= 0 16236E+01

Figure 16--Grid in Physical Plane

14-22

It is noted that the creation of a grid in the mapped plane utilizing polar coordinates fails to generate an acceptable grid in the physical plane due to the covering of more than the upper half plane in the latter by the upper half plane in the mapped plane. In order to overcome this shortcoming, various schemes were tried, including the addition of a tail to the mushroom in the physical plane, also the utilization of a quarter circle in the mapped plane instead of a semi-circle. The results of these attempts are presented in Figures 17-19. The introduction of a singularity downstream of the mushroom is evident. It became evident that the intermediate utilization of the Kutta-Joukowsky transformation to map the real axis onto a circle is not appropriate for the point-wise Schwarz-Christoffel transformation. Rather, the grid is to be generated by Cartesian coordinates in the mapped plane, as shown in Figures 20 and 21.
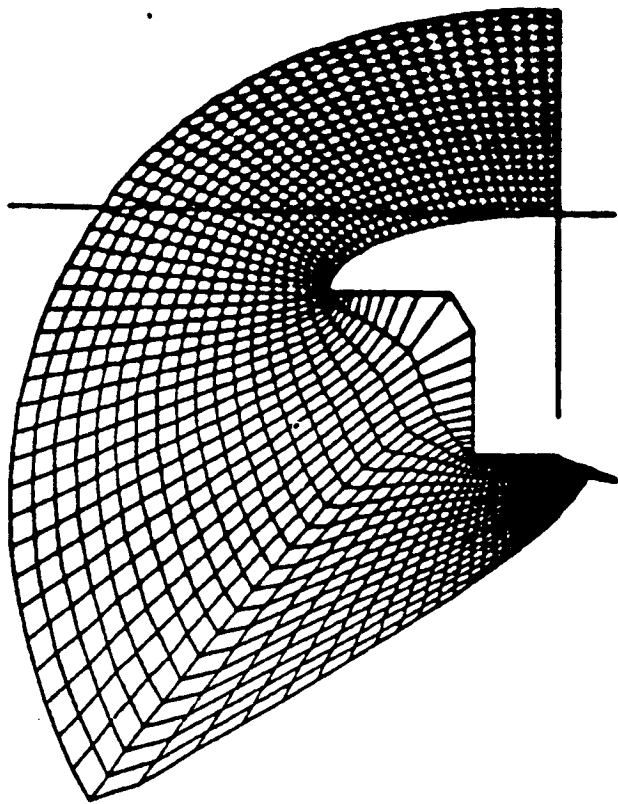
Figure 17- Quarter Circle, No Tail
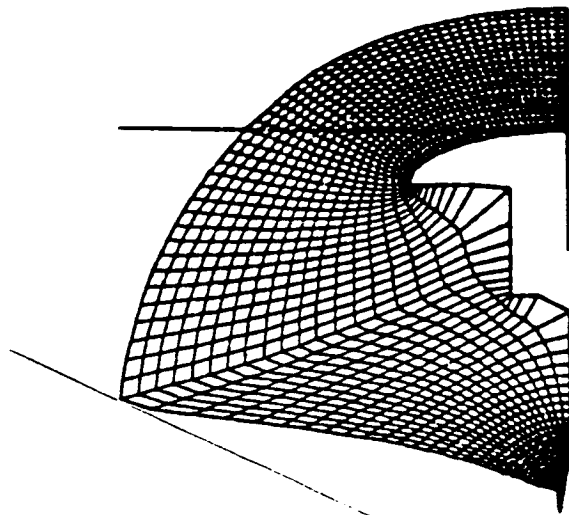
Figure 18-Quarter Circle, Tail
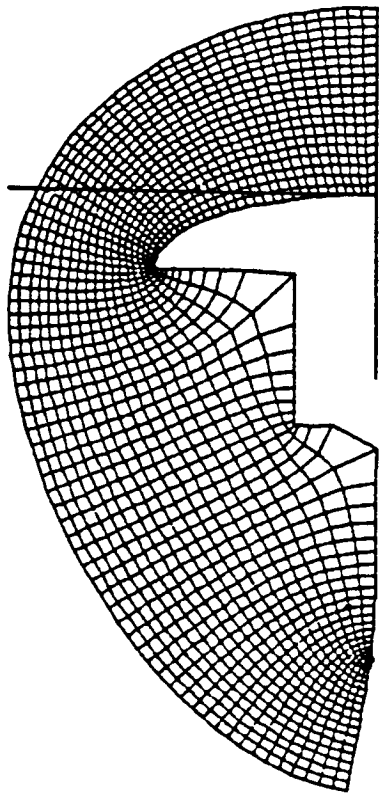
FIGURE 19 - SEMI CIRCLE, TAIL
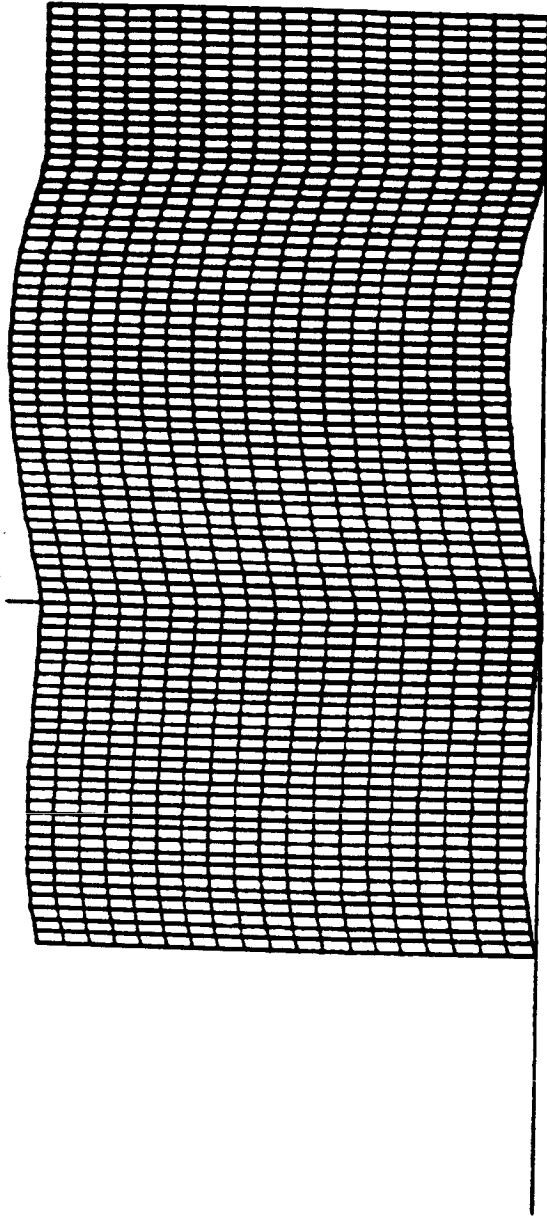
Figure 20--Cartesian Grid Construction in Mapped Plane
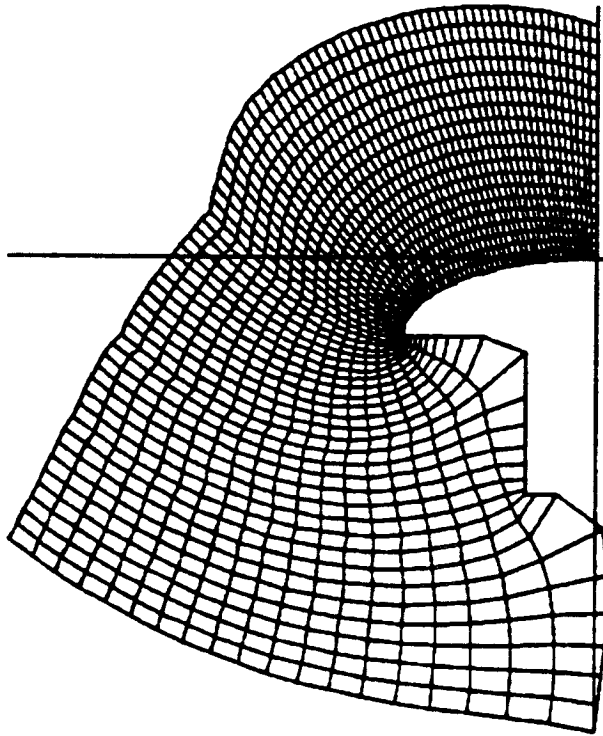
FIGURE 21 - TAIL, CARTESIAN COORDINATES

XN= 0.80888E+01

4. Transformation of a Square

As noted earlier, it was desired to transform a simpler shape in order to gain insight into the transformations. A square was chosen for this effort, and the results are presented in the following figures. Trends similar to those observed for the mushroom are noted.

Figure 22 shows the square after the first Karman-Trefftz transformation has been applied. One corner has been smoothed out, and one remains. Figure 23 shows the square after the second corner has been removed. It is this latter shape which is utilized in Figure 24 for the construction of a polar grid, similar to what was done in Figure 5 for the Aerobrake body. Figure 25 shows the grid after the first inverse transformation, and Figure 26 shows the final grid in physical space.

The original square is shown in Figure 27, with the point-numbering convention for the Point-wise Schwarz-Christoffel transformation. After moving point 1 down to the real axis, the square takes on the shape shown in Figure 28. The next transformation moves point 2 up to the real axis, as shown in Figure 29; followed by the positioning of point 3 on the real axis as shown in Figure 30. Again the Kutta-Joukowsky transformation is applied, giving the near-circle shown in Figure 31. The polar grid is constructed in Figure 32, and the first inverse transformation yields the grid shown in Figure 33. However, Figure 34, which displays the result of the second inverse transformation, indicates trouble in that the grid begins to overlap itself. Figure 35, the grid in physical space, shows that, although the square has been successfully mapped back into physical space, the grid has not fared so well. Apparently, Figure 33 contains the explanation for the failure. Part of the grid in Figure 33 lies at an angle with the real axis which is greater (More negative) than that of line segment 2-3. It is this portion of the grid which cannot be successfully mapped back into physical space, probably because it is on another branch. Again, a Cartesian coordinate system is constructed in Figure 36, corresponding to Figure 20 for the Aerobrake body. When this is mapped back into physical spcae, Figure 37 results. The odd shape of this grid at infinity is clearly unacceptable. Instead, a tail is added to the square, both upstream and downstream, and the results are shown in Figures 38 and 39. The rear side of the square has been "lost" again, due to the interpolation scheme, as can be seen by comparing Figures 38 and 39.
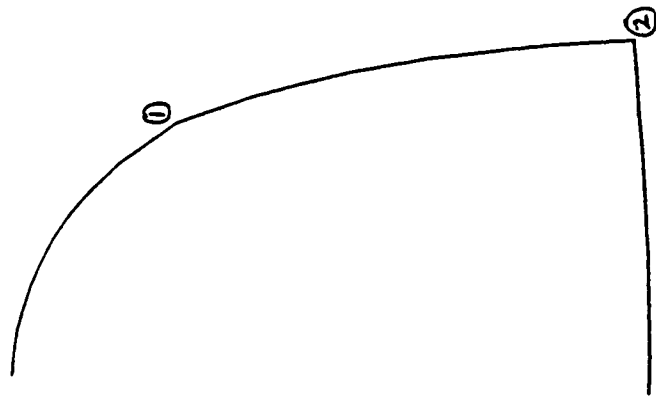
KARMAN TREFFTZ

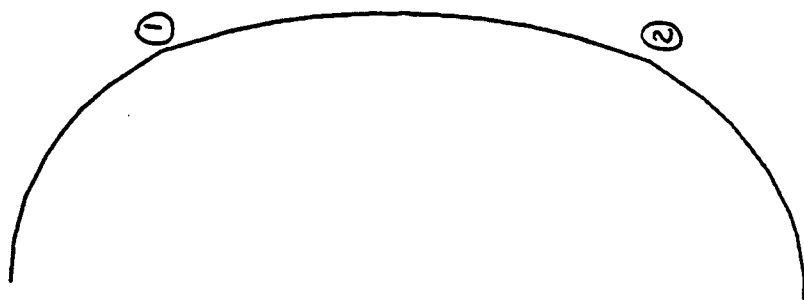Figure 22—Square after First Karman-Trefftz Transformation

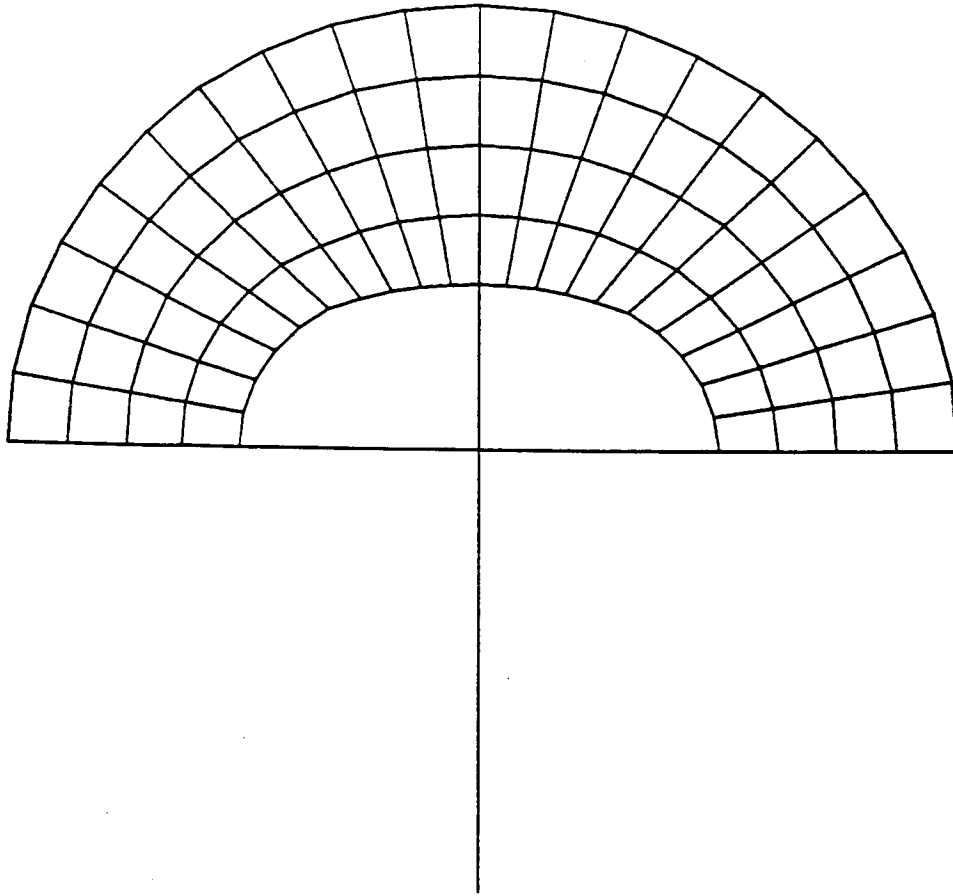Figure 23--Result of Second Transformation
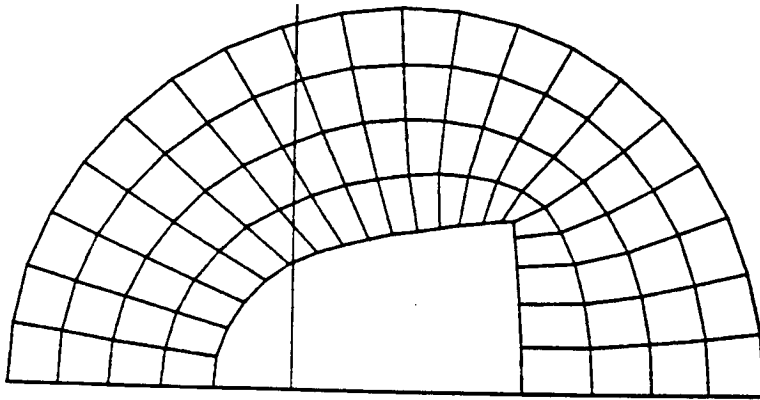
Figure 24--Grid Construction in Mapped Plane
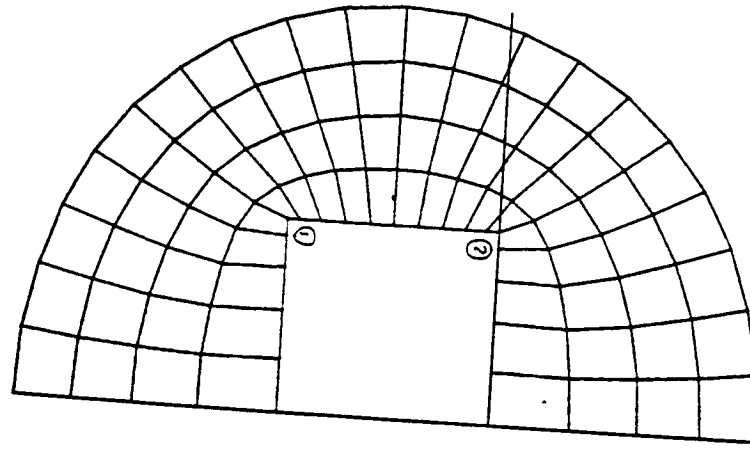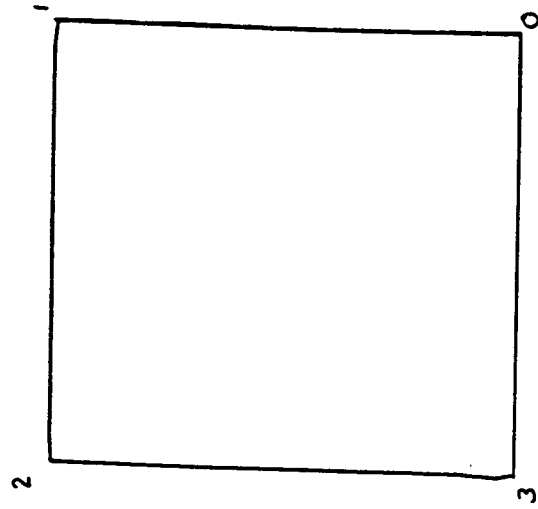
Figure 25--Grid after First Inverse Transformation

Figure 26--Grid in Physical Space

Point-Wise Schwarz-Christoffel

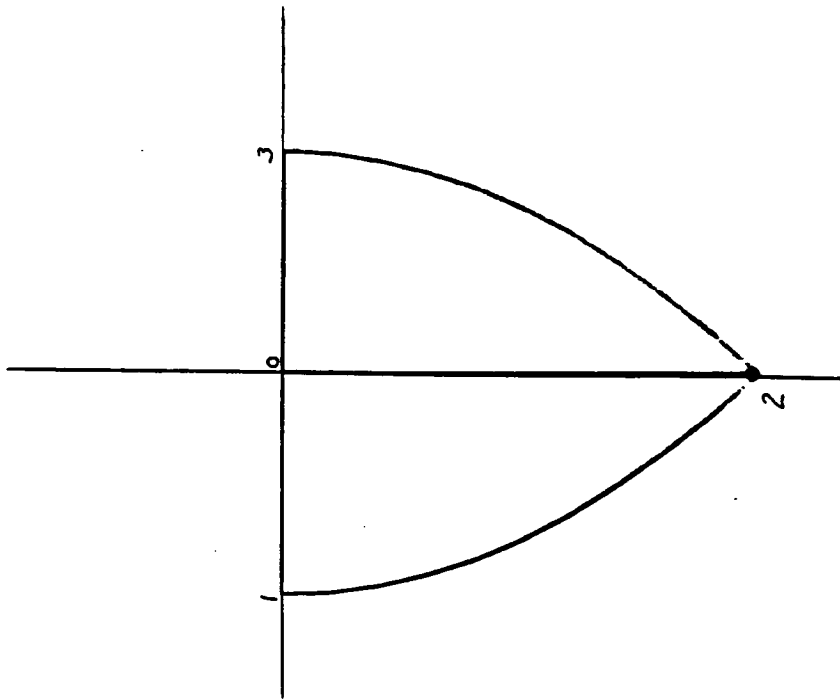Figure 27--Orientation of Square for Point-Wise Schwarz-Christoffel Transformation
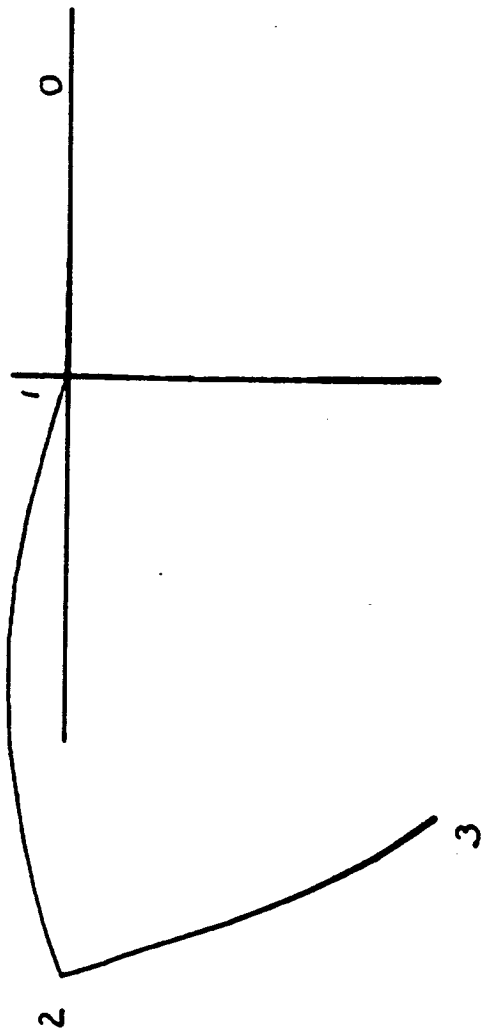
Figure 28--Result of First Transformation
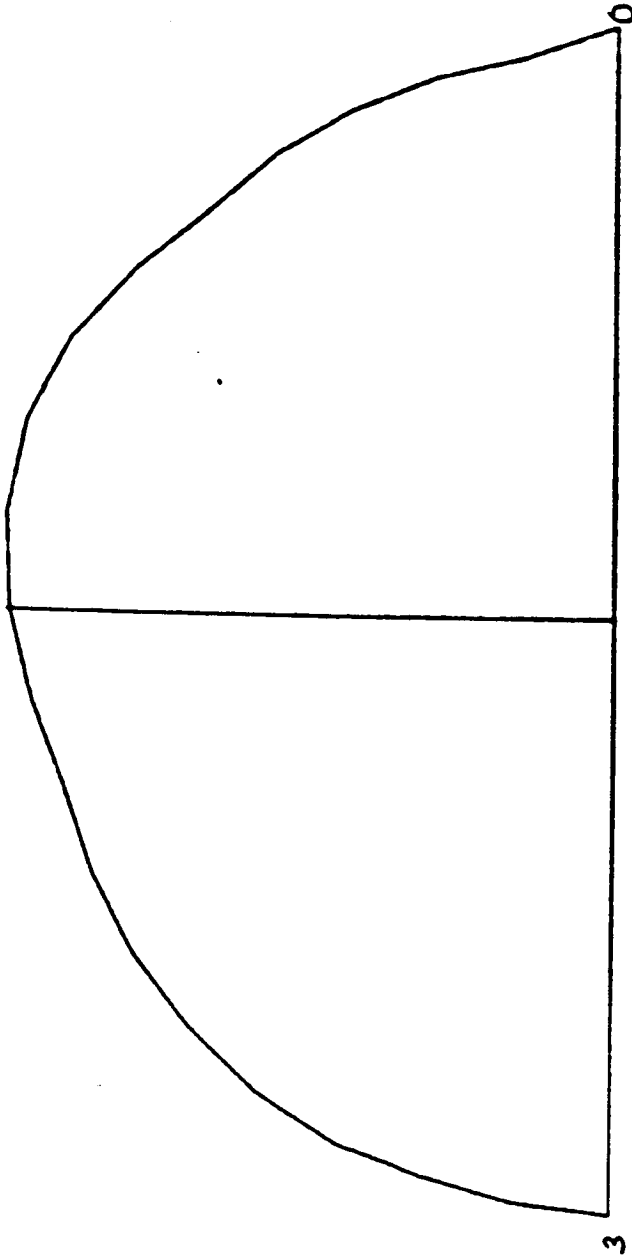
Figure 29--Result of Second Transformation

Figure 30--Result of Third Transformation

FIGURE 31 - AFTER KUTTA-JOUKOWSKY TRANSFORMATION
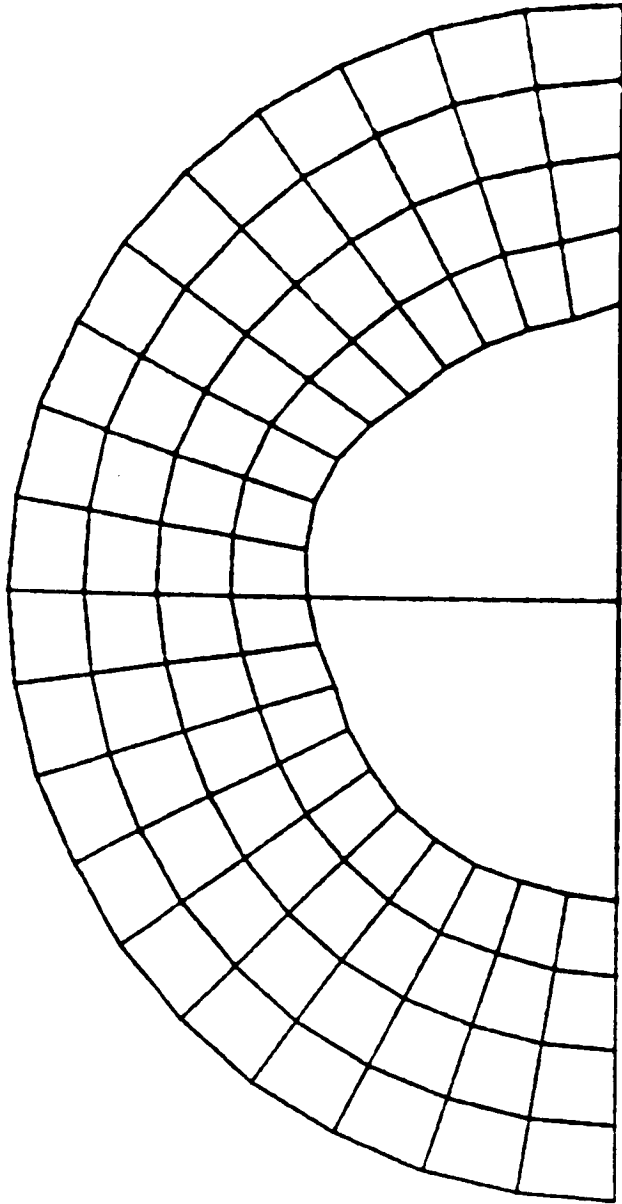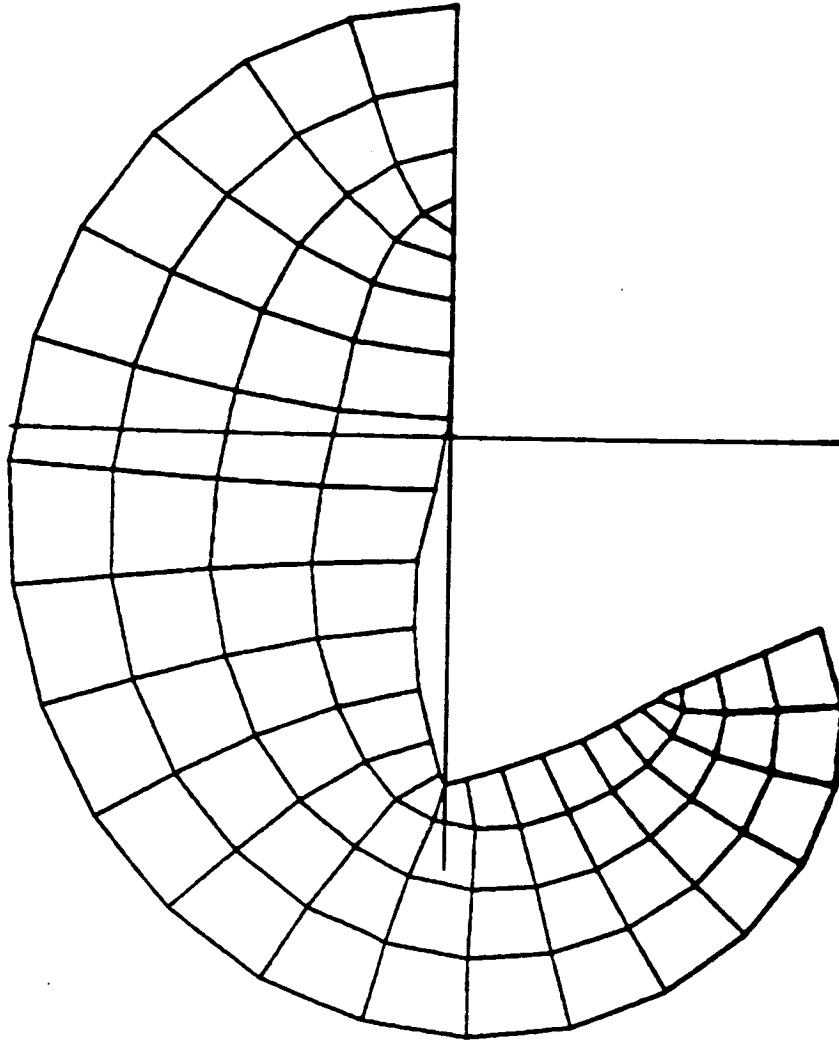
DEN= 0.20915E+01

Figure 32--Polar Grid Generation

14-40

DEN= 0.28042E+01

Figure 33--Polar Grid after First Inverse Transformation

14-41
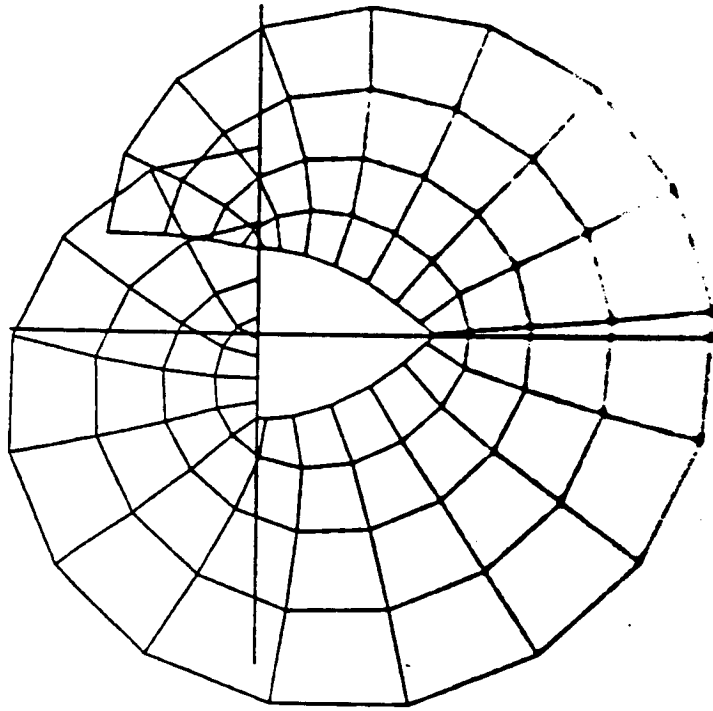
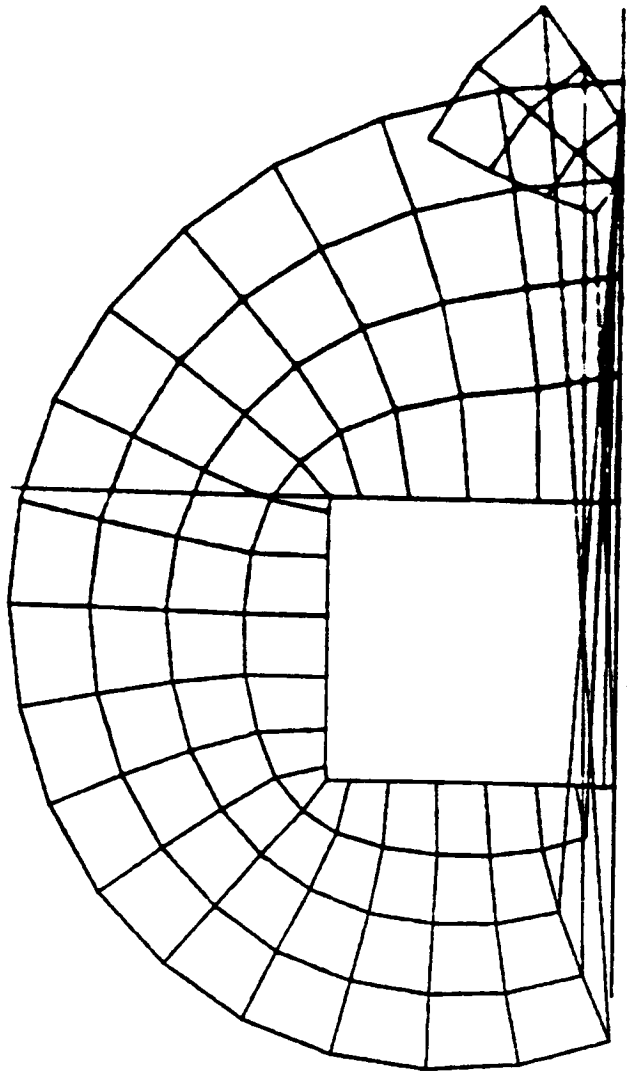Figure 34—Polar Grid after Second Inverse Transformation

Figure 35--Polar Grid in Physical Space
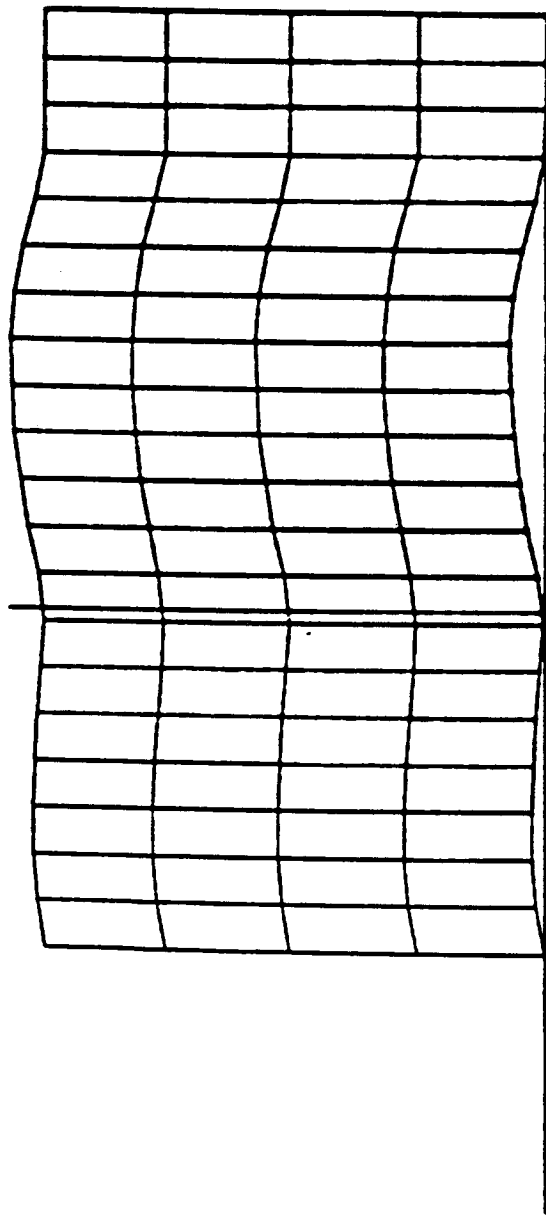
DEN= 0.18047E+01

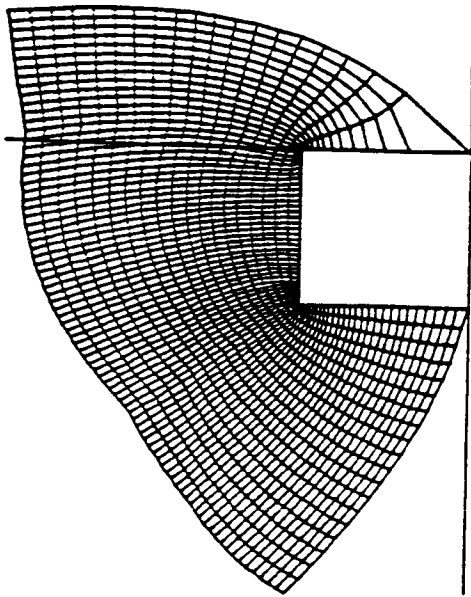Figure 36--Cartesian Grid Generation in Mapped Space

DEN= 0.2923IE+01

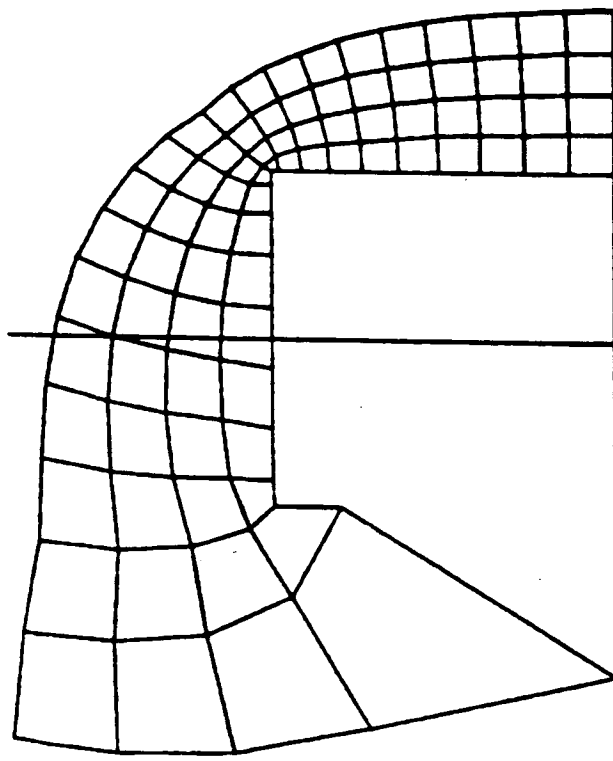Figure 37--Cartesian Grid in Physical Plane

14-45

DEN= 0.17912E+01

Figure 38--Cartesian Grid for Square with Tails in Physical Space,
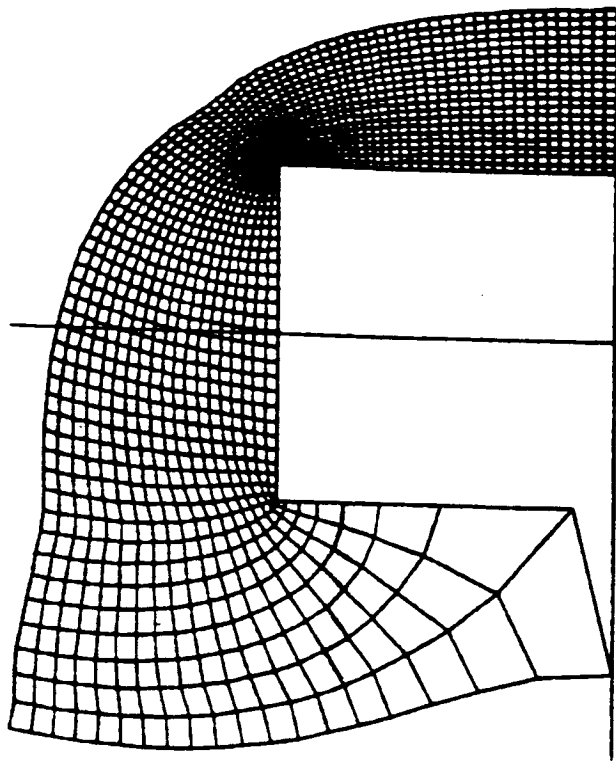Coarse Mesh

14-46

DEN= 0.17912E+01

Figure 39--Cartesian Grid for Square with Tails, Fine Mesh

5. Conclusions and Recommendations

Table 1 summarizes the advantages and disadvantages of the two transformations. It is seen that both have complementary advantages and disadvantages. One disadvantage of both transformations which is listed in Table 1 refers to poor resolution at concave corners. This is not a serious disadvantage, at least for the flow past the Aerobrake Body, because the flow in this region is of lesser interest.

Based on the results, the following recommendations are offered:

1.   The Karman-Trefftz transformation appears to be best suited to finite bodies around which the entire flow field is desired. The type of mesh which results under this transformation is an "O" mesh.

2.   The point-wise Schwarz-Christoffel transformation appears to be best suited to infinite bodies, or finite bodies with long trailing wakes. The type of mesh results under this transformation is a "C" mesh.

Transformation	Advantages	Disadvantages
Karman-Trefftz	1. Clustering at Convex Corners 2. Orthogonal at Front & Rear 3. Well-Shaped at Infinity	1. Not Orthogonal on Stem 2. Poor Resolution at Concave Corners
Point-Wise Schwarz-Christoffel	1. Clustering at Convex Corners 2. Orthogonal Everywhere	1. Odd-Shaped at Infinity 2. Poor Resolution at Concave Corners

Table 1--Comparison of the Two Transformations

6. References

1. Li, C.P., 1985, Numerical Procedure for Three-Dimensional Hypersonic Viscous Flow over Aerobrake Configuration, NASA TM58269.

2. Moretti, G., 1976, Conformal Mappings for Computations of Steady, Three-Dimensional, Supersonic Flows, Numerical/Laboratory Comp. Methods in Fl. Mech., A.A. Pouring and V.I. Shah, Ed., ASME, pp. 13-28.

3. Hall, D.W., 1980, A Three-Dimensional Body-Fitted Coordinate System for Flow Field Calculations on Asymmetric Nosetips, Numerical Grid Generation Techniques, NASA Conf. Publ. 2166.

4. Spiegel, M.R., 1964, Complex Variables, McGraw-Hill.